Environmental Engineering and Management Journal

November 2021, Vol. 20, No. 11, 1759-1771
http://www.eemj.icpm.tuiasi.ro/; http://www.eemj.eu

"Gheorghe Asachi" Technical University of Iasi, Romania

DESORPTION KINETICS OF THERMAL ENHANCED SOIL VAPOR EXTRACTION ON HYDROCARBON REMOVAL IN SIMULATED AND MODIFIED SOILS

Ling Zhu[1*], Yujie Yang[1,2], Ziyu Yang[1], Yimin Sang[1]

[1]Beijing Institute of Petrochemical Technology, Beijing, 102617, China
[2]Beijing University of Technology, Beijing 100124, China

Abstract

Different from the traditional research on the influencing factors, the paper combined the thermal enhanced extraction technology with desorption kinetics to study the removal effect of hydrocarbon contaminated soil in depth. Research for the effect of gas flow rate, gas water content (GWC), soil water content (SWC) and modified soil on the removal rate of hydrocarbon pollutants. The physical and chemical properties of soil restoration were detected by FT-IR, BET and SEM-EDS. The calculated kinetic constant (k) in LDF kinetic equation was basically stable after the gas flow rate more than 80 mL·min^{-1}. When GWC raised to 15%, the numerical changed obviously. While SWC increased to 10%, R^2 (R^2=0.9849) reached maximum. Among the modified soils, k decreased from 0.01487 to 0.00283 and the desorption rate remained around 99% as acid modified soil with short desorption time (from 330 to 270 min). Compared with the experimental data, the LDF kinetic equation was more suitable for the study of single-component kinetic process. Freundlich kinetic equation was fit for complex-component (water-contained) kinetic process. The changes in soil structure, porosity and elements caused by acid, alkali and salt modification had an impact on the rate of thermally enhanced soil vapor extraction (T-SVE) to remediate contaminated soil. At the end of remediation in the acetic acid modified soil, the average concentration of pollutants was reduced from 127569 to 848 mg/kg, corresponding to 99.3% of mass removal.

Key words: desorption kinetics, hydrocarbon contaminated soil, modified soil, thermally enhanced soil vapor extraction

Received: December, 2020; Revised final: April, 2021; Accepted: May, 2021; Published in final edited form: November, 2021

1. Introduction

Environmental problems caused by hydrocarbon contamination of soil are well known. Organic contaminants are directly toxic to living organisms (Valavanidis et al., 2006), so the functioning of both natural (Volkmar et al., 1998) and agricultural systems (Dawson et al., 2008) can be altered. It can effectively affect the soil, which leads to the destruction of plants and the inhibition of soil bioactivity (Eisenhauer et al., 2011). In addition, such pollution may pose a threat to human health (Ly et al., 2016), which rules out residential or commercial use in these areas. Hydrocarbon contaminated soil is a complex mixture of organic compounds, such as gasoline, diesel, paraffin and asphalt, etc. Due to these characteristics, it is necessary to develop appropriate technologies for the remediation of hydrocarbon contaminated soil (Islam et al., 2014). Remediation techniques which can be categorized to some branches, such as soil vapor extraction (SVE) (Hamby et al., 1996), bioremediation (BR) (Albergaria et al., 2006; D'Imporzano et al.,2019), soil venting (Mcalexander et al., 2015), composting (Huang et al., 2016), thermal treatment (Croat et al., 2020; Huang et al., 2016; Pop et al., 2018), chemical oxidation (Mcalexander et al., 2015; Tsitonaki et al., 2010; Doula et al., 2019) and incineration (Leuser et al., 1990). BR and SVE are the

* Author to whom all correspondence should be addressed: e-mail: zhuling75@bipt.edu.cn, zhuling7519@163.com; Phone: +86-10-81294271; Fax: +86-10-81292291

most common methods. The cost of BR is low but the cycle is long. SVE is typically effective for the removal of contaminants from higher permeability portions of the vadose zone (Carroll et al., 2012). Although SVE was a very effective approach, its limitations were recognized gradually over time. It is difficult to completely remove the pollutants, and the properties of the soil are relatively high. In many cases, thermal remediation is an effective and reliable method to reduce the concentration of soil pollutants (remove contaminants in a short time), hence born of T-SVE remediation technology. T-SVE remediation is a combination of SVE and thermal remediation, which is a potential alternative by delivering heat to the soil system, increasing the permeability of the substrate by adding steam and removing VOCs (Yu et al., 2015).

Recent studies of thermal remediation for contaminated soil had been focused on the comparison of influencing factors. There are few studies on the thermally enhanced desorption kinetics combined with numerical modeling for the designing and optimization of the remediation process for in situ applications. The influencing factors of T-SVE remediation of semi-volatile petroleum hydrocarbons in contaminated soil were studied and the removal process was described by thermal desorption kinetics (Yu et al., 2017). Experiments proved that temperature has a decisive effect on the removal process of organic matter in the soil. Wang (2018) found that the more complex the pore structure of the soil, the shorter the desorption time of volatile organic compounds (VOCs) was.

The paper expresses a research from different angles comprising gas flow rate, gas water content (GWC) and soil water content (SWC) on the thermal desorption efficiency of hydrocarbon contaminated soil. The LDF and Freundlich equation is used to describe the desorption process, calculate the kinetic parameters and go into the application range of desorption kinetics. The effects of acid, alkali and salt soil modification on soil remediation were studied by gas chromatograph. The physical and chemical properties of soil restoration before and after soil restoration are detected by an infrared spectrometer (FT-IR), specific surface area and pore volume tester and scanning electron microscope (SEM). The obtained results can provide a reference for the industrial design of T-SVE for the remediation of hydrocarbon contaminated soil.

2. Materials and method

2.1. Simulated and modified soil samples preparation

The soil was selected from sandy soil on the campus. In the sampling process, the garbage and impurities were screened out to avoid its impact on the experiment. 20-mesh sieve (0.850mm soil particle size) was used to screen the soil samples. The soil sample was taken to the 114 laboratory for drying. The drying temperature was selected at 150℃ and the drying time was 6 hours. The original moisture in the soil sample was removed to eliminate the influence of the original moisture in the soil sample on the experiment. Then mixed with gasoline (C_5~C_{12}, aliphatic hydrocarbons, cycloalkanes and aromatic hydrocarbons) uniformly. The specific operation method: Using precision electronic balance in the 206 laboratories, measuring 10g after drying of the soil, and then take a certain amount of hydrocarbon pollutants by the moving liquid gun (the experiment selected the gasoline as laboratory reagents of different hydrocarbon pollutants), and then mixed with soil and placed in the refrigerator of 112 laboratory for aging seal a week. The concentration of gasoline in polluted soil is 22.5% m/m. Under the optimal experimental conditions, the same amount of acetic acid, ammonia water and sodium chloride were added to the soil to make into acidic soil, alkaline soil and saline soil. The same amount of hydrocarbon pollutants was poured into these soils to deliberate the remediation rate of T-SVE under different soil conditions.

2.2. T-SVE Treatment experiment

The schematic diagram of the experimental system is illustrated in Fig. 1. The system consists of a T-SVE reactor, condenser system, temperature controller, stove and gas detector system.

The VOCs concentration in the outlet was continuously monitored by a gas chromatograph (GC-3000-115), which was equipped with a total hydrocarbon filling column and an FID detector. The corresponding desorption time was taken as the evaluation parameter when the HC concentration in the gas dropped to 800 $mg \cdot m^{-3}$. The detection conditions were: FID temperature: 130°C; inlet temperature: 175°C; column temperature: 80°C; total pressure: 400kPa; intake pressure: 101kPa.

Under the experimental conditions of soil volume at 80 mL, the desorption efficiency of aeration rate (40, 60, 80 and 100 $mL \cdot min^{-1}$), GWC (0%, 5%, 15%, 25%) and SWC (0%, 5%, 10%, 15%) on the T-SVE processing were investigated. The extraction gas flow rate of 80 $mL \cdot min^{-1}$ was selected.

2.3. Characterization of soils

Fourier infrared spectrometer (FT-IR) absorbance spectra was recorded on a Bruker Tensor 27 spectrometer, the experimental condition is 4000-400cm^{-1} and the scanning speed is at a resolution of 4cm^{-1} (Wang et al., 2012). Each collected spectrum was measured in ambient air against that of pure KBr as a background spectrum. Scanning electron microscope (SEM) and energy dispersive spectroscopy (EDS) were characterized in the soil at the aim of assessing the distribution form of soil particles (Zhu et al., 2013). Nitrogen sorption isotherms at liquid-nitrogen temperature were obtained on a Quanta Chrome NOVA2000 gas sorption analyzer. The Brunauer-Emmett-Teller (BET) surface area was calculated using the experimental points at a relative pressure of P/P_0=0.05-0.95.

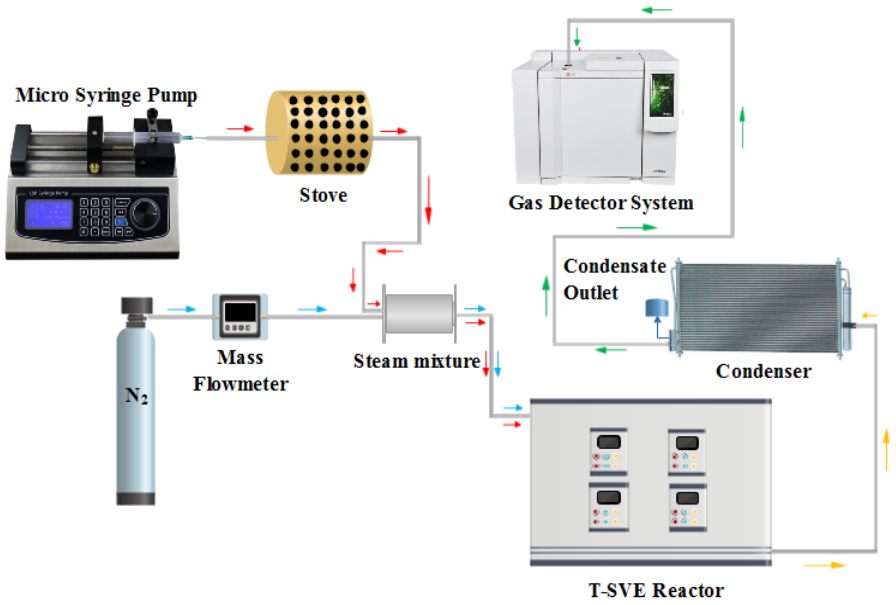

Fig. 1. Flow diagram of the experimental device

The internal surface area of micropores was obtained from the *T*-plot method and the micropore size distribution was calculated from the Horvath-Kawazoe method (Hu et al., 2020).

2.4. Desorption kinetics models

Gauss model was used to fit the functional relationship between the concentration of HC in the extracted gas and the desorption time of T-SVE. The calculation method is shown in (Eq. 1) (Li, 2018).

$$C_g = C_{g0} + \frac{A}{w\sqrt{\pi/2}} \cdot e^{-2\left(\frac{t-t_c}{w}\right)^2} \quad (1)$$

where: the C_g is the concentration of HC in the extracted gas after treatment, mg·m^{-3}; C_{g0} is the concentration of HC in the original state, mg·m^{-3}; t is the treatment time, min; t_c is the desorption time at which the HC concentration reached a maximum in the extracted gas, min; A and w are desorption kinetic constants, min^{-1}.

When $t = t_c$, $C_{g,max}$ reaches a maximum value in (Eq. 2) .

$$C_{g,max} = C_{g0} + A / \left[w\left(\sqrt{\pi/2}\right)\right] \quad (2)$$

where: the $C_{g,max}$ is the maximum concentration of HC in the extracted gas, mg·m^{-3}.

Under the condition of 120°C, hydrocarbon components are less likely to be decomposed thermally. The linear driving force (LDF) model can be used to calculate the desorption kinetics of organic pollutants in soil. This model describes a series of gases/steam on carbon adsorption materials (activated carbon, carbon molecular sieves and silica gel) in general, the calculation method is shown in (Eq. 3).

$$\eta = M_t / M_e = 1 - e^{-kt} \quad (3)$$

where: the η is the relative removal rate; M_t is the desorption amount at time t, mg; M_e is the equilibrium desorption amount, mg; k is the desorption kinetic constant, min^{-1}.

The Freundlich kinetic equation is used to analyze the process of a series of reaction mechanisms, which is mainly used to describe the process of exponential decay on adsorption energy with the increase of surface saturation. The calculation method is shown in (Eq. 4) (Arroyo et al., 2019; Li et al., 2017).

$$\ln C = B + D \ln t \quad (4)$$

where: the C is the concentration of organic matter in soil, mg·m^{-3}; B and D are desorption kinetic constants, min^{-1}.

3. Results and discussion

3.1. Influence factors of T-SVE in simulated soil

3.1.1. Effect of extraction gas flow rate

Extraction gas flow rate is an important parameter for T-SVE due to its direct impact on the mass transfer occurring during the remediation process (Li et al., 2019). The experiment was carried out without considering the effect of GWC and SWC on treatment efficiency. The effect of extraction gas flow rate on the hydrocarbon-contaminated soil processing is shown in Fig. 2 and Table 1. In the paper, the curve of the concentration and time in Fig. 2a were integrated to obtain the desorption amount M_t and M_e. According to the total hydrocarbon concentration of the soil obtained by the TPH (total petroleum hydrocarbon) infrared analyzer. The actual purification efficiency of the thermal desorption and

the theoretical time of the T-SVE treatment were calculated in line with the LDF model. The results were shown in Table 1 and Fig. 2b. The fitting curve of the Freundlich equation was shown in Fig. 2c.

It can be seen from Fig. 2(a) that the curve of HC concentration in the extracted gas with time was a parabola of fundamental symmetry. The mass transfer of hydrocarbon components within soil was simultaneously affected by their volatilization, adsorption and desorption (Zhao et al., 2019). The hydrocarbon components of the soil removed fast then slow and the tailing occurred in the end of thermal desorption (Poppendieck et al., 1999). It can be attributed to the exist of free energy on the soil surface. When the water vapor in the extraction gas was saturated, molecular attraction still existed on the soil surface, which leaded to some hydrocarbon pollutants remaining in the soil. With the evaporation of water vapor, hydrocarbon pollutants were also carried away from the soil. Fig. 2b is the relation curve between desorption treatment time and removal rate of organic pollutants in the soil. Under different experimental conditions, the trend of organic matter concentration in the soil was basic unanimously. After 380 min treatment, the removal rate of organic matter was over 93%. The results of the fitting curve with the LDF equation were shown in Table 1. The calculated kinetic constant (k) was increased from 0.00635 to 0.00868, k was basically stable after the extraction gas flow rate more than 80 mL·min^{-1}. The conclusions were related the kinetic equation to fit the removal process of contaminants in the soil by Ma (2011). When the rate was upgraded from 40 mL·min^{-1} to 100 mL·min^{-1}, meanwhile, the treatment time (t_{exp}) was down to 330 min. The time required for the experiment was basically the same as the time required for the LDF fitting calculation. Thus, it can be seen that the removal process of organic pollutants in the soil accords with the LDF dynamic equation model under the influence of single factor of extraction gas flow rate. The time that the Freundlich equation calculated was slightly larger than the LDF.

Furthermore, the higher the extraction gas flow rate is, the faster the gas is purging. Some of soil particles are migrated, they are entrained by the gas to move toward the air outlet, which interfere with soil remediation. The kinetic constant was fundamentally consistent at 80 mL·min^{-1} and 100 mL·min^{-1}. Consequently, when studying the influence of other factors on the removal efficiency of organic pollutants in soil, 80 mL·min^{-1} extraction gas flow rate would be appropriate.

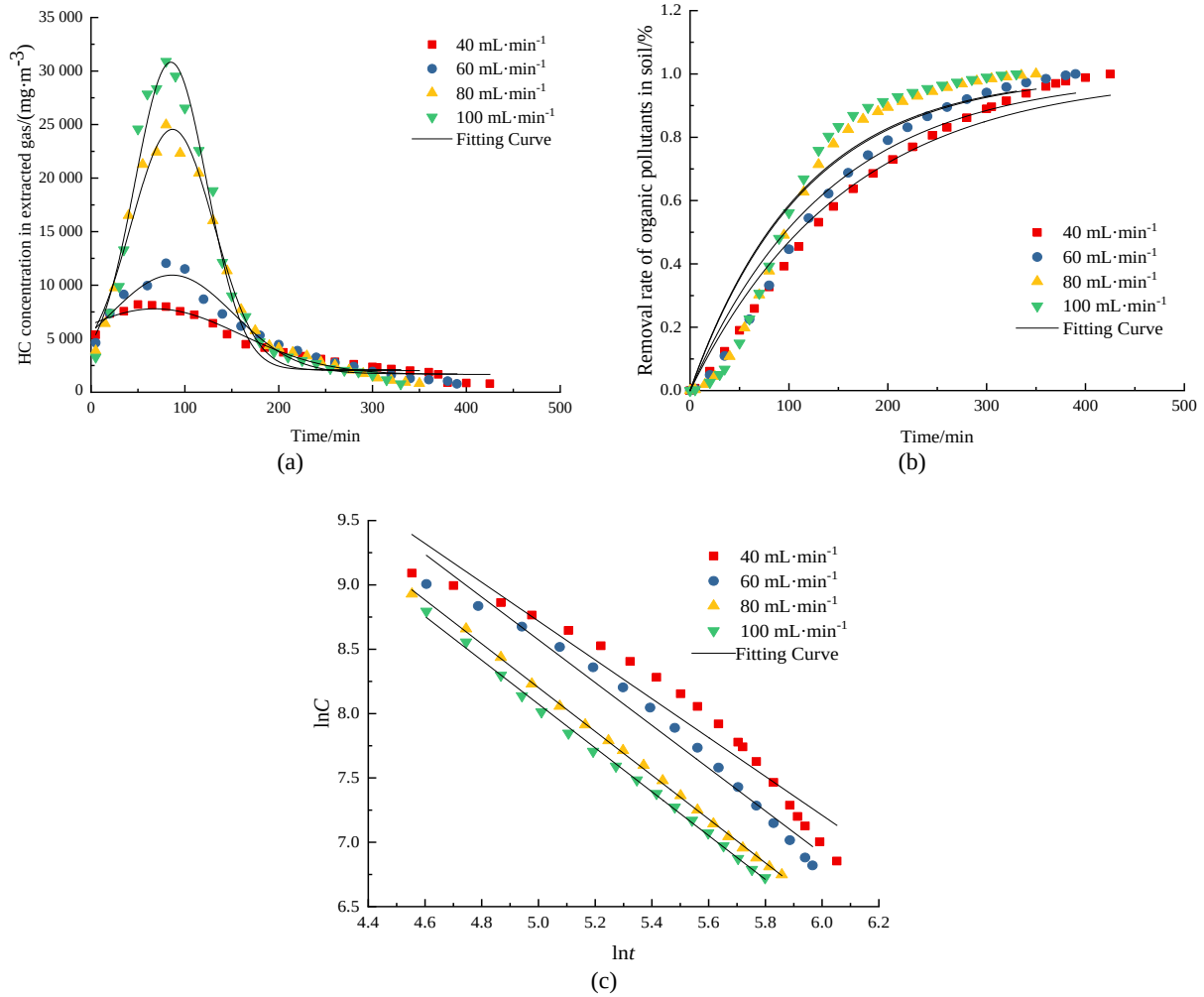

Fig. 2. Effect of extraction gas flow on simulated contaminated soil processing: (a) Curve of HC concentration in extracted gas; (b) Curve of time and removal rate; (c) Curve of time and HC concentration in soil

Table 1. Parameters of the fitted equation and experimental results at different extraction gas flow rates

Extraction gas flow rate /(mL·min^{-1})		***40***	***60***	***80***	***100***
Gauss	***R^2***	0.957	0.946	0.979	0.978
	C_{max}/ (mg·m^{-3})	7785.50	10938.62	24568.87	28840.87
Experimental result	***C_s/(mg·kg^{-1})***	948	916	852	832
	η_{exp}/%	93.2	93.4	96.5	94.1
	t_{exp}/min	425	380	350	330
LDF equation	***k/min^{-1}***	0.00635	0.00720	0.00868	0.00882
	R^2	0.977	0.969	0.941	0.918
	t_{sim1} /min	423	377	336	321
	Deviation rate/%	-0.47	-0.79	-4.00	-2.72
Freundlich equation	***Fitting equation***	y=16.261-1.5085x	y=16.884-1.6622x	y=16.231-1.6142x	y=16.589-1.7032x
	R^2	0.9427	0.9763	0.9863	0.9980
	t_{sim2} /min	510	417	356	373
	Deviation rate/%	20.0	9.7	1.7	-7.8

3.1.2. Effect of GWC in extracted gas

The effect of GWC in soil remediation is shown in Fig. 3 and Table 2. The experiment was carried out with gas flow rates (80 mL·min^{-1}) and SWC (0%) of the soil. When there was no vapor water in the extraction gas, the hydrocarbon components were adsorbed on the soil particles resulting in a low fugacity value. It affected the overall volatilization rate in the pore of soil. After the addition of vapor water to the extracted gas, the removal efficiency was significantly enhanced. When the GWC was 15%, the fitting and experiment time was the shortest, 119 minutes and 105 minutes respectively, and the processing efficiency also reached the highest value of 97.9%. The dynamic constant was 4 times value of anhydrous steam. This had to do with the fact that water molecule was polar. It was easier to combine with the surface components of the soil particles. When the GWC sustainable added to 25%, the removal speed geared down and the processing time lengthened to 240 minutes.

Water vapor from the extracted gas could occupy the pores of the soil and cause blockages. It reduced the flow volume of gas in the soil and decreased the permeability of the soil. On the contrary, it increased the desorption time of organic pollutants. The experimental results proved that the appropriate GWC had a positive effect on the removal of hydrocarbon pollutants.

The LDF kinetic equation is a dynamic process describing the control of the diffusion mechanism. It is not suitable for describing the diffusion of particles and liquid membranes. When GWC was raised to 15%, the absolute deviation between the experimental time and the fitting time reached 13.3%. Since the Freundlich equation is appropriate for the fitting of multi-factor processing, the water would have a "stripping" effect on the pollutants during to evaporation between the organic pollutant components (Fang, 2016). From the fitting results of the Freundlich equation, it can be seen that when the GWC was 15%, the time required for the fitting calculation was basically the same as the actual time, the absolute value of the relative deviation was 3.8% and the fitting degree was superior.

3.1.3. Effect of SWC on hydrocarbon contaminated soil

The effect of SWC on hydrocarbon contaminated soil is shown in Fig. 4 and Table 3. The experiment was carried out with gas flow rates (80 mL·min^{-1}) and GWC (10%) of the soil. SWC affects the volatilization rate, effective porosity and air permeability of organic matter in the soil, thus impacting the in situ thermal desorption (Jiao et al., 2019). When the SWC added to 5%, the treatment time was curtailed from 350 min to 195 min. While the SWC progressively increased to 10%, the peak appearance time was 290 min, which was 95 min later than the SWC of 5%. The constant of the dynamic constant (k=0.01849) was 2.1 times of the value without moisture. However, the film of water was formed between the pores of the soil, the membrane resistance would affect the further desorption of the HC component.

In addition, especially in the later stage of treatment, the concentration of organic matter in the soil retarded and the desorption resistance ascended. He et al. (2008) proved the SWC to be the main factor influencing the removal efficiency of the organic pollutants from soils by SVE. The results of this paper showed that SWC has optimum value. The SWC within a narrow range is beneficial to the dissipation of heat and promotes the volatilization process, so that more organic pollutants can be evaporated from the soil. In moist soil, contaminants are more likely to desorb from the soil surface. Owing to water molecules are polar, they are more easily combined with organic components in the soil than non-polar molecules. As can be seen from Fig. 4, under the conditions of the present research, the optimum removal efficiency was achieved when the SWC was 10% from the view of the removal rate.

To the results of LDF equation fitting, the R^2

value of LDF decreased from 0.9849 to 0.8505 and the absolute value of deviation increased from 17.2% to 18.5% as SWC among 10% to 15%. In contrast with the fitting results of Freundlich, the absolute value of the deviation rate was only 6.7% at 15%, the fitting degree was comparatively higher than the LDF equation. So the removal of organic pollutants in hydrocarbon contaminated soil is more in line with the Freundlich equation model under the condition that the water contained in the soil.

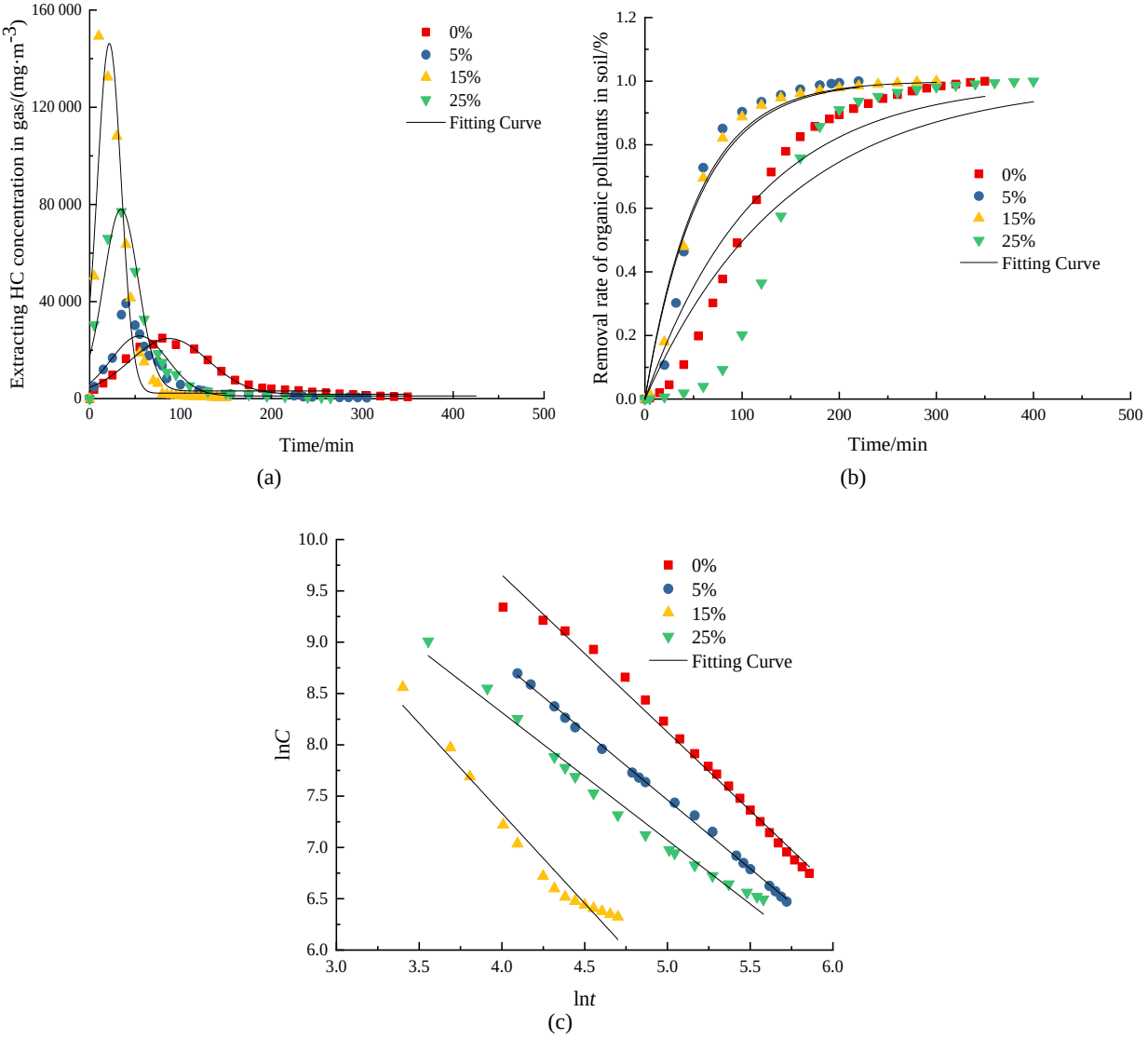

Fig. 3. Effect of GWC in extracted gas on simulated contaminated soil processing: (a) Curve of HC concentration in extracted gas; (b) Curve of time and removal rate; (c) Curve of time and HC concentration in soil

Table 2. Parameters of the fitted equation and experimental results on different GWC

GWC/%		**0**	**5**	15	25
Gauss	R^2	0.979	0.936	0.928	0.979
	C_{max}/ (mg·m^{-3})	24568.87	33624	140235.08	74671.29
Experimental result	C_s/(mg·kg^{-1})	852	738	519	647
	η_{exp}/%	96.5	94.3	97.9	95.4
	t_{exp}/min	350	312	105	240
LDF equation	k/min^{-1}	0.00868	0.03319	0.03683	0.02142
	R^2	0.94100	0.93112	0.96058	0.97448
	t_{sim1}/min	336	258	119	196
	Deviation rate/%	-4.0	-17.3	13.3	-18.3
Freundlich equation	***Fitting equation***	y=16.231- 1.6142x	y=13.115-1.2093x	y=14.351-1.755x	y=13.288-1.2434x
	R^2	0.9863	0.9872	0.9619	0.9839
	t_{sim2}/min	356	291	101	267
	Deviation rate/%	1.7	-6.7	-3.8	11.3

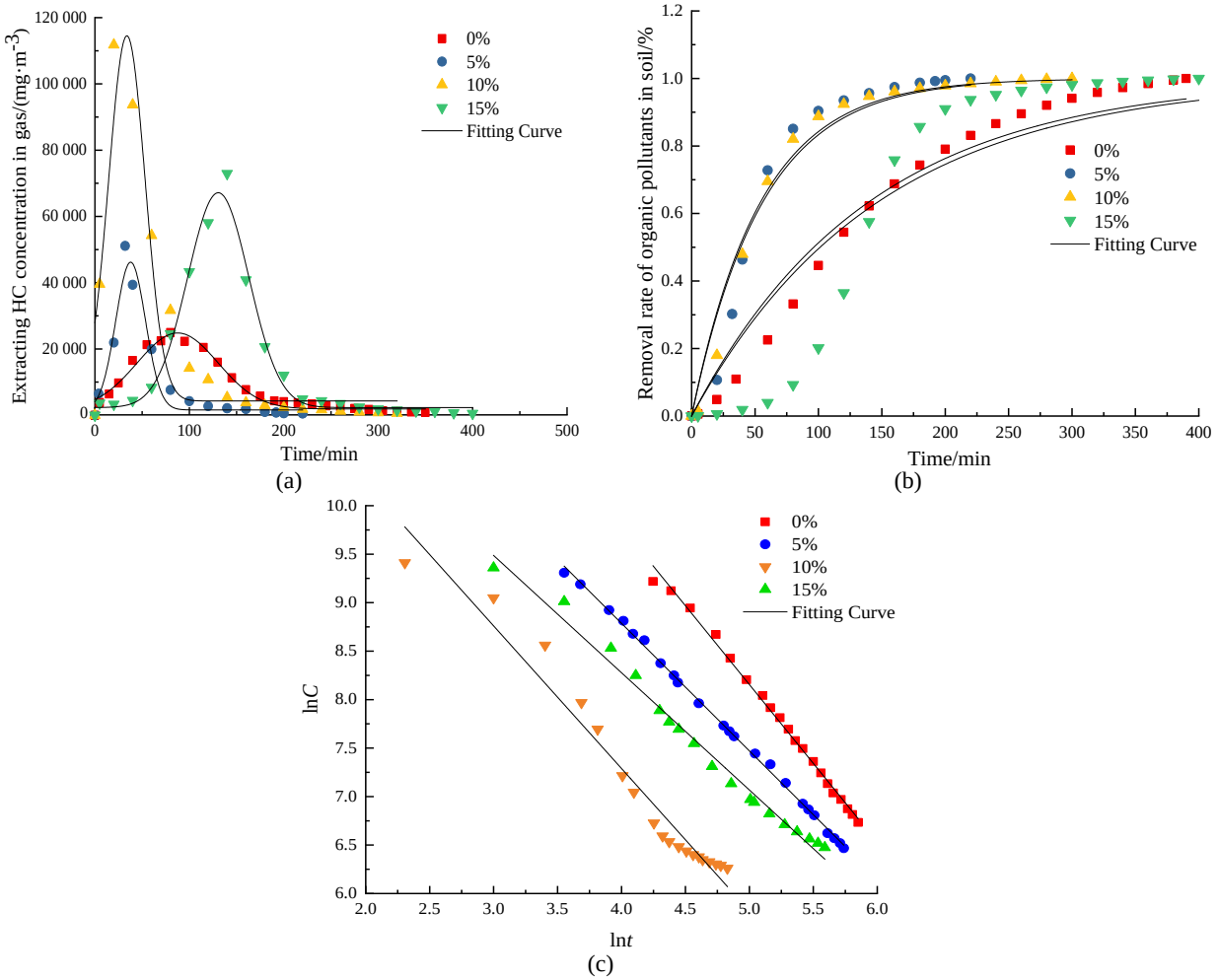

Fig. 4. Effect of SWC on simulated contaminated soil processing: (a) Curve of HC concentration in extracted gas; (b) Curve of time and removal rate; (c) Curve of time and HC concentration in soil

Table 3. Parameters of the fitted equation and experimental results on different SWC

SWC/%		***0***	***5***	***10***	***15***
Gauss	R^2	0.979	0.948	0.862	0.978
	C_{max}/ (mg·m^{-3})	24568.87	46362.86	114497.59	67387.49
Experimental result	C_s/(mg·kg^{-1})	852	646	782	1984
	η_{exp}/%	96.5	96.9	99.5	93.1
	t_{exp}/min	96.5	195	290	390
LDF equation	k/min^{-1}	0.00868	0.01792	0.01849	0.00684
	R^2	0.94100	0.9593	0.9849	0.8505
	t_{sim1}/min	336	180	240	318
	Deviation rate/%	-4.0	-7.7	-17.2	-18.5
Freundlich equation	Fitting equation	y=16.231-1.6142x	y=11.648-0.9461x	y=13.021-1.0982x	y=13.382-0.9888x
	R^2	0.9863	0.9415	0.9232	0.9554
	t_{sim2}/min	356	200	224	348
	Deviation rate/%	1.7	2.6	-7.7	-6.7

3.2. Desorption of hydrocarbon in modified soils

The changes in soil structure, porosity and elements caused by acid modification, alkali modification and salt modification have an impact on the rate of T-SVE to remediate hydrocarbon contaminated soil. The soil modification was carried out under the conditions of ventilation rate of 80 mL·min^{-1}, GWC of 15% and SWC of 10%. Some volume of water solution of acetic acid, ammonia and sodium chloride were added into the contaminated soil drop by drop and shaken quickly. The effects of modified soil on pollutant removal are shown in Fig. 5 and Table 4. In Fig. 5(a), the concentration and time curves of the modified soils were integrated. From the figures, the remediation rate of normal soil was obviously higher than that of other modified soils. According to the experimental results of dynamics in Table 4, the kinetic constant k (k=0.01487) value in LDF equation of acid modified soil was the largest that

reflected the fastest removal rate, reaching 99.3%. The time deviation between theoretical data and actual data showed that the deviation of normal soil was at least 4%, acid, alkaline and salt modified soil was 18.2%, 13.2% and 5.6% respectively. The deviation of the Freundlich equation was 1.7%, 1.8%, 5.8% and 5.0%, respectively. The results showed that the overall remediation rate of salt soil was the lowest. The comparison of the removal rate was: acid soil > alkaline soil >salt soil. A previous modeling study has shown that pH is more effective in the removal rate of hydrocarbon pollutants compared to heating time during T-SVE process, and thus higher removal efficiency can be achieved by changing the pH (Yu et al., 2019). When pH>6, some hydrocarbon groups will stick to the soil particles tightly, thus extending the remediation time. In the acid environment, the surface and structure of the soil can be changed, the adsorption of hydrocarbon components in the soil can be weakened, so the remediation time is relatively short. The salt-modified environment makes the soil easier to harden and makes it less permeable to water and air, thus affecting the removal rate of pollutants.

3.3. Characterization of acetic acid modified soil

(1) FT-IR

Typical FT-IR spectra for each of the studied soils are presented in Fig. 6. The composition of the soil was evaluated by using the peak heights at 1500-400 cm^{-1} and 4000-1000 cm^{-1}. Fig. 6(a) showed the infrared spectrum of the normal soil, from which it can be clearly seen that the characteristic peak was relatively dense in fingerprint areas and scattered in functional groups. Soil composition is more complex, including olefin, aromatic hydrocarbon, alcohol, alkane, ketone, carboxylic acid and other inorganic components.

The absorption peak at 1000-650 cm^{-1} was the result of bending vibration outside the CH surface of alkenes and aromatics based on differences in the abundance of certain functional groups. The peaks around 1624 cm^{-1} were lead to the stretching vibration of the N=N and C=C double bonds. The peaks around 3421 cm^{-1} were caused by OH (polymolecular association, carboxyl group) and NH (dissociation) stretching vibration.

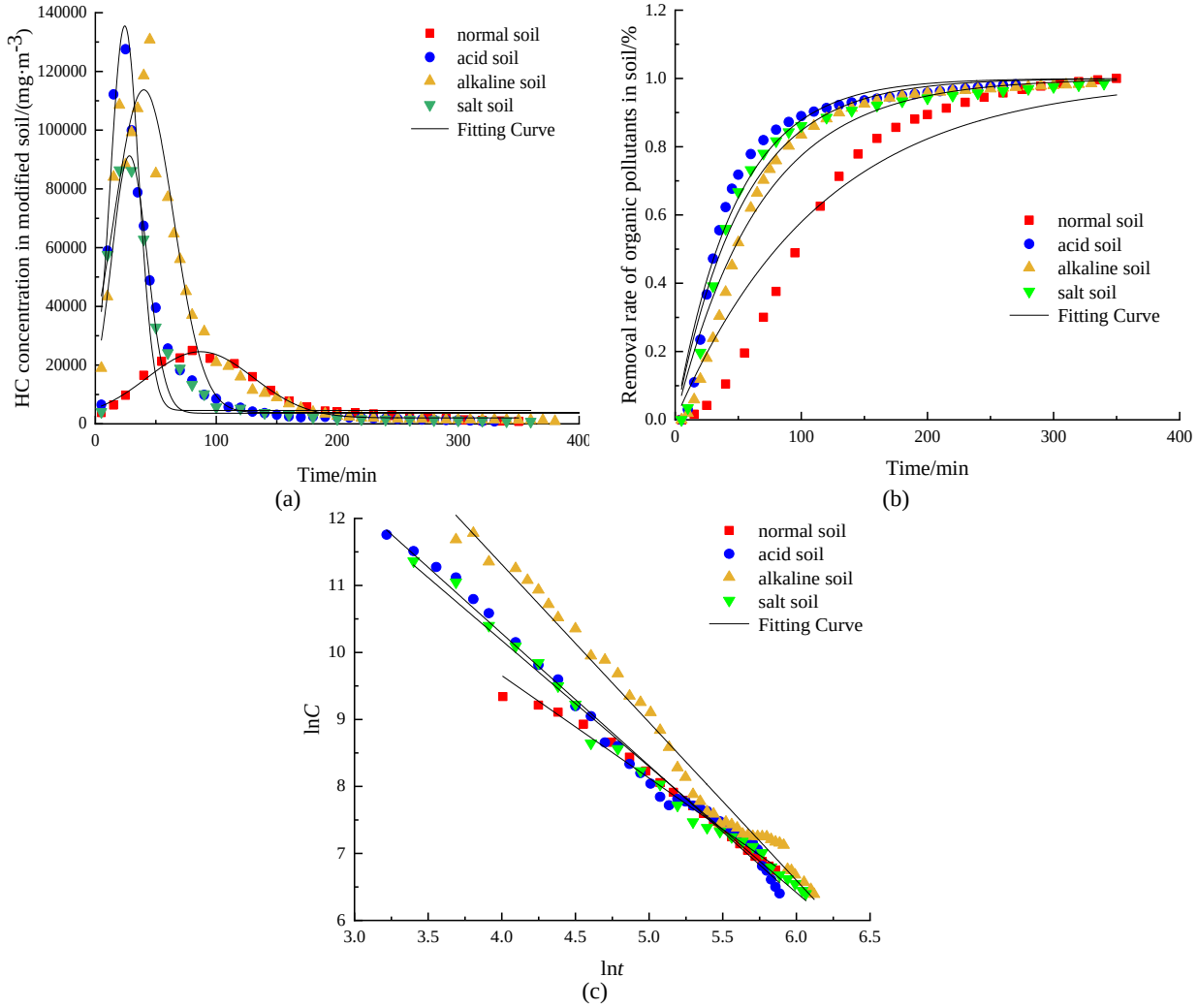

Fig. 5. Effect of the removal rate of pollutants in modified soils: (a) Curve of HC concentration in modified soils; (b) Curve of time and removal rate; (c) Curve of time and HC concentration in soils

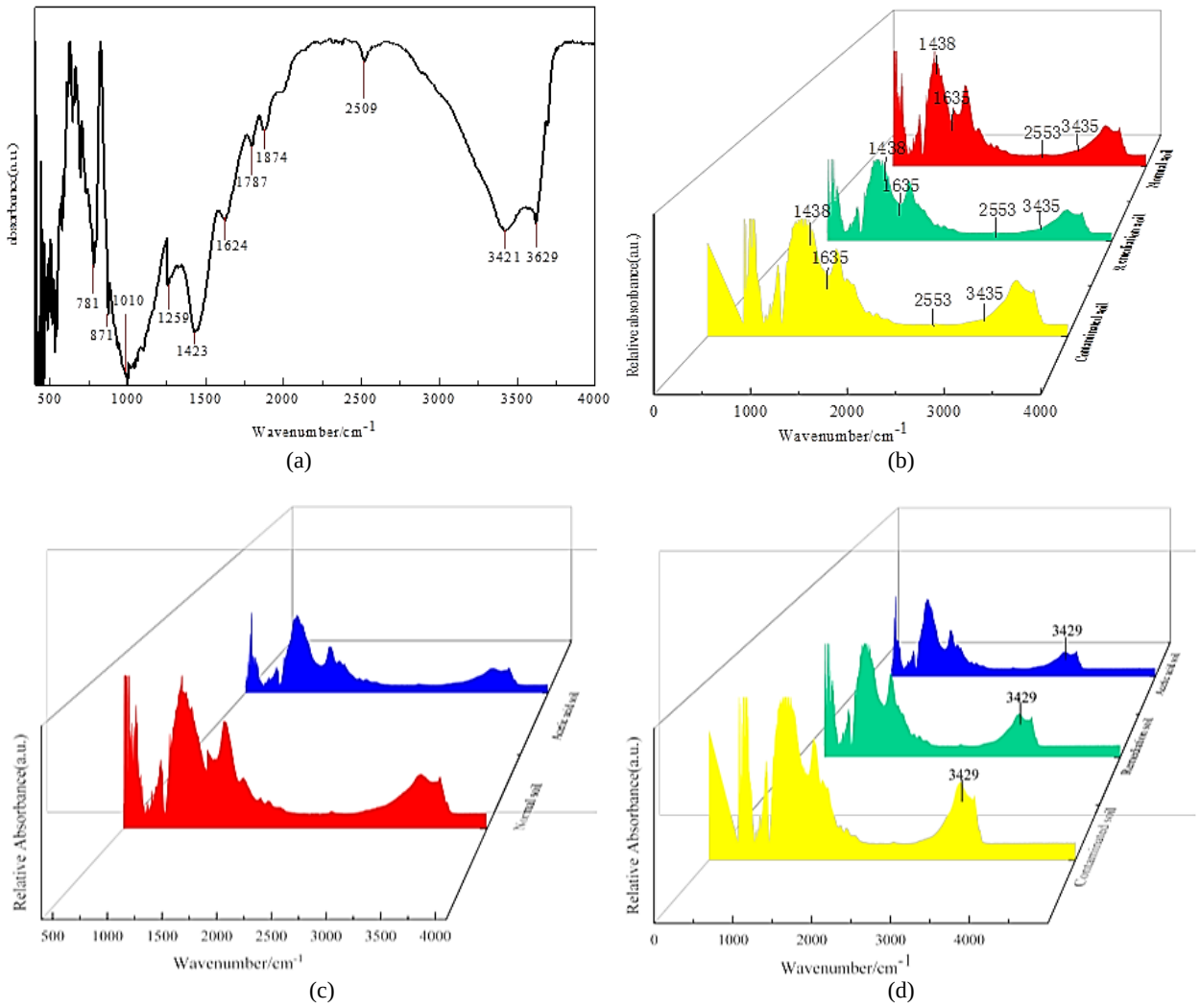

Fig. 6. Infrared spectrum contrast diagram of soils samples: (a) nrmal soil; (b) acetic acid soil; (c) normal soil and acetic acid contaminated soil; (d) before and after remediation under the acetic acid soil

Table 4. Parameters of the fitted equation and experimental results on modified soils

modified soils		***normal***	***acid***	***alkaline***	***salt***
Gauss	R^2	0.979	0.948	0.920	0.909
	C_{max}/ (mg·m^{-3})	24568.87	127569	130806	86368
Experimental result	C_s/(mg·kg^{-1})	852	848	867	793
	η_{exp}/%	96.5	99.3	99.3	99.1
	t_{exp}/min	350	330	380	360
LDF equation	k /min^{-1}	0.00868	0.01487	0.00210	0.00283
	R^2	0.9410	0.9659	0.9671	0.9697
	t_{sim1} /min	336	270	330	340
	Deviation rate/%	-4.0	-18.2	-13.2	-5.6
Freundlich equation	***Fitting equation***	y=16.231-1.6142x	y=20.745-2.3577x	y=18.178-1.9736x	y=17.700-1.8809x
	R^2	0.9863	0.9834	0.9891	0.9889
	t_{sim2} /min	356	324	402	378
	Deviation rate/%	1.7	-1.8	5.8	5.0

Fig. 6(b) displayed the typical FT-IR spectra for each of the studied soils like contaminated soil and remediation soil. It can be seen from the figure that the three soil peaks were almost the same, but the specific light transmittance was different at the wave number of 1438 cm^{-1}, 1635 cm^{-1}, 2553 cm^{-1} and 3435 cm^{-1}, especially at 2553 cm^{-1}. With the addition of pollutants, light transmittance is significantly enhanced. Nevertheless, the transmittance decreased obviously after remediation. The comparison of infrared spectra between normal soil and acetic acid contaminated soil is formulated in Fig. 6(c). The results indicated that

the difference of functional groups in the soil with acetic acid was small. The comparison of infrared spectrum without gasoline, with gasoline and after remediation under the condition of acetic acid modified soil is showed in Fig. 6(d). The results were generally consistent with those of normal soil during the same contaminants added.

(2) SEM-EDS

SEM image of the normal soil used for the EDS compositional analysis is shown in Fig. 7. This was done by mapping the SEM/EDS, which revealed that the distribution of soil particles and parameters such as soil surface structure. It can be seen that there existed many micro-pores on the surface of the soil, which was the typical feature of the soil particle distribution.

As the SEM images of acetic acid soil and contaminated soil mixed with acetic acid and gasoline at a magnification of 2,000 times shown in Fig. 7(e)(f). By comparing acetic acid soil with unmodified soil, it can be clearly seen that the pores on the surface of the normal soil were denser after being magnified, while the same magnification (Fig. 7e) could be obviously seen that the surface of acetic acid soil was more flat with fewer pores. The specific surface area of soil increased after the addition of gasoline because of acetic acid causing some of the pores in the soil surface block and collapse. SEM coupled with EDS was used to assess the element distribution within the soil samples. The EDS results as shown in Fig. 8 demonstrate that C, O, Na, Mg, Al, Si, K, Ca and Fe exist in acetic acid soil. In this regard, in addition to Si and Al were considered as the main atoms constituting soil samples (Haberhauer et al., 1999). More precisely, the content of Si and Al is the highest. The contents of other metal elements increased except K and Fe.

(3) BET

The specific surface area, pore volume and average particle size of normal soil, contaminated soil and remediation soil under the condition of normal soil mixed with acetic acid reagent are shown in Table 5. It can be seen from the table that the specific surface area, pore volume and particle size of contaminated soil without modification by acetic acid tended to be smaller. The value increased from 0.809 m^2g^{-1}(contaminated soil) to 1.314 m^2g^{-1} (remediation soil) after remediation but remained small compared to the normal soil.

Some pores in the soil surface were occupied by hydrocarbon components. This phenomenon resulted in a decrease in specific surface area and pore volume. Meanwhile, some pollutants were removed and the original pores were reduced after restoration. In the end, the specific surface area and pore volume were recovered.

After adding pollutants to the soil modified by acetic acid, the surface area and pore volume increase compared with the normal soil. It was clear that the vast majority of pollutants on the surface was located in the microspores of the soil. The BET indicated a significant dilation in the specific surface area from 1.238 m^2g^{-1} (normal soil) to 1.537 m^2g^{-1} (contaminated soil) (Mora et al., 2014). There is a positive correlation between specific surface area and the absorbability of soil. This model was based on the application of the Langmuir equation to the first and subsequent layers of adsorbate on the surface (Zhang et al., 2011).

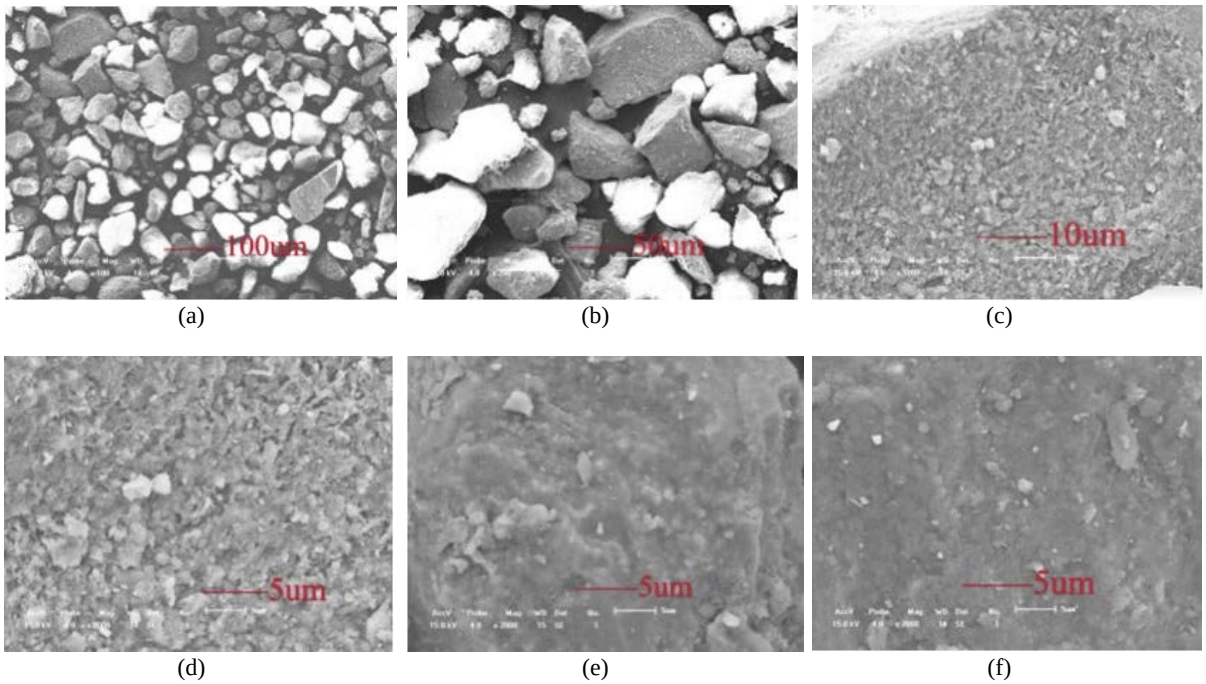

(a) (b) (c)

(d) (e) (f)

Fig. 7. Diagram on SEM of soil samples: (a) normal soil (×0.1K); (b) normal soil (×0.2K); (c) normal soil (×1K); (d) normal soil (×2K); (e) acetic acid soil (×2K); (f) contaminated soil (×2K)

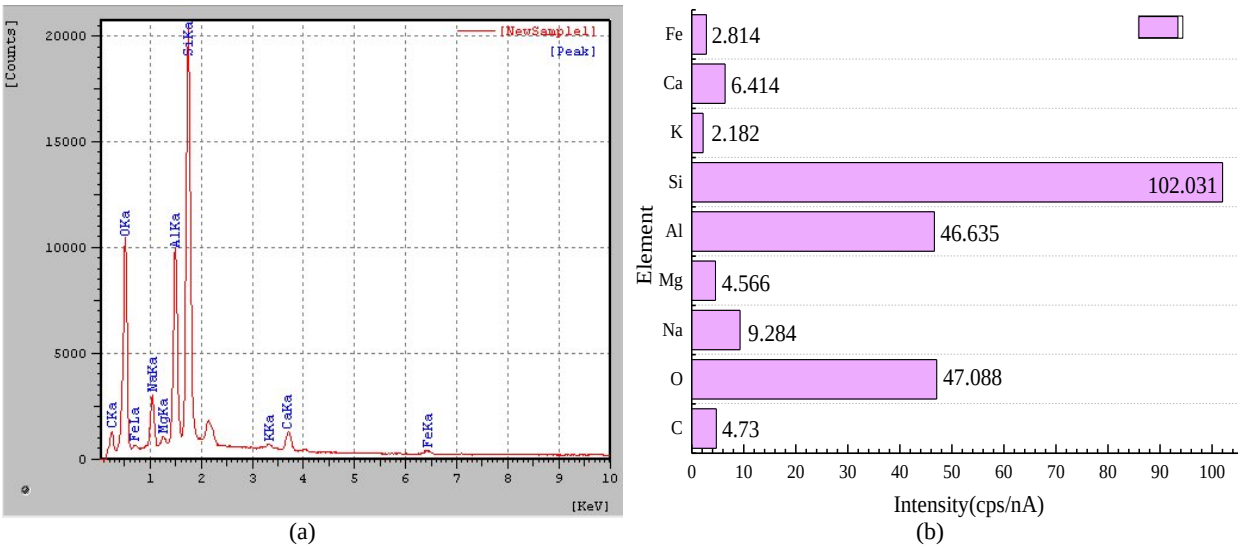

Fig. 8. Diagram of element content in acetic acid soil: (a) EDS diagram of acetic acid soil; (b) Distribution of elements in soil samples

Table 5. Soil specific surface area and porosity

Reagent	*State*	*Specific surface area m^2/g*	*Porosity 10^{-9} m^3/g*	*Particle size 10^{-3} mm*
Space	normal	2.325	7.635	19.231
	contaminated	0.809	3.772	18.910
	remediation	1.314	3.729	17.968
Acetic acid modify	normal	1.238	2.520	19.113
	contaminated	1.537	4.278	18.248
	remediation	1.769	2.915	17.818

Under the same conditions, the absorbability was not easy to desorption. The addition of acid corroded the internal structure of soil, which increased the soil porosity, thus resulting in the increase of soil specific surface area. The experimental results were in agreement with those of SEM. The porosity and particle size of remediation soil decreased owing to the process of desorption heating and sintering.

4. Conclusions

The results revealed the optimal processing conditions: gas flow rate of 80 mL·min^{-1}, GWC of 15% and SWC of 10%. The ventilation rate exceeded 80 mL·min^{-1}, the removal rate of hydrocarbons (93.9%) was basically balanced. Freundlich equation could be described the diffusion process in surface and liquid film of the pollutants better. In the study of modified soils, the fitting degree (R^2) of the two equations all reached the standard of 95%, even up to 99%.

Among the modified soils, the acid modified soil had the lowest absolute deviation of Freundlich equation (1.8%), the highest removal efficiency (99.3%) and least desorption time (324 min). The consequence indicated that the addition of acid could effectively improve the removal efficiency of pollutants in the soil.

Under the condition of acetic acid modified soil, contaminated soil obtained larger BET surface area (1.537m^{2}g^{-1}) and pore size (4.278×10^{-9}m^{3}g^{-1}) comparing with normal soil. The thermal desorption efficiency was improved and the experimental results of acid soil modification accord with the desorption kinetic equations.

Acknowledgements

This work was supported by grants from Support Project of High-level Teachers in Beijing Municipal Universities in the Period of 13th Five-year Plan——Beijing Municipal College "Great Wall" Scholars Projects (CIT&TCD20190314), the Award Cultivation Foundation from Beijing Institute of Petrochemical Technology (Project No. BIPTACF-003), and SINOPEC's Projects (320109).

References

Albergaria J., Alvim-Ferraz M., Delerue-Matos C., (2006), Remediation efficiency of vapour extraction of sandy soils contaminated with cyclohexane: Influence of air flow rate, water and natural organic matter content, *Environmental Pollution*, **143**, 146-152.

Arroyo.S., Rosano-Ortega G., Martínez-Gallegos S.,Pérez-Armendáriz B., (2019), Hydrocarbon removal from diesel-contaminated soil through reused activated carbon adsorption, *Environmental Engineering and Management Journal*, **18**, 1917-1925.

Carroll K., Oostrom M., Truex M., Rohay V., Brusseau M., (2012), Assessing performance and closure for soil vapor extraction: Integrating vapor discharge and impact to groundwater quality, *Journal of Contaminant Hydrology*, **128**, 71-82.

Croat S., DeSutter T., Casey F., O'Brien P., (2020), Phosphorus sorption and desorption in soils treated by thermal desorption, *Water, Air, and Soil Pollution*, **231**, 2161-2169.

Dawson J., Huggins D., Jones S., (2008), Characterizing nitrogen use efficiency in natural and agricultural ecosystems to improve the performance of cereal crops in low-input and organic agricultural systems, *Field Crops Research*, **107**, 89-101.

D'Imporzano G., Re I., Spina F., Varese C., Puglisi E., Spini G., Gramellini C., Zaccanti G., Beltrametti F., Bava A., Adani F., (2019), Optimizing bioremediation of hydrocarbon polluted soil by life cycle assessment (LCA) approach, *Environmental Engineering and Management Journal*, **18**, 2155-2162.

Doula M., Zorpas A., Inglezakis V., Navvaro J, Bilalis.D,, (2019), Optimization of heavy polluted soil from olive mill waste through the implementation of zeolites, *Environmental Engineering and Management Journal*, **18**, 1297-1309.

Eisenhauer N., Milcu A., Sabais A., Bessler H., Brenner J., Engels C., Scheu S., (2011), Plant diversity surpasses plant functional groups and plant productivity as driver of soil biota in the long term, *PLoS ONE*, **6**, e16055, https://doi.org/10.1371/journal.pone.0016055.

Fang C., (2016), *Composition of organic pollutant in wastewater discharged from delayed coking plant and its influence on treatment efficiency*, PhD Thesis, Chengdu University of Technology, China.

Haberhauer G., Gerzabek M., (1999), Drift and transmission FT-IR spectroscopy of forest soils: an approach to determine decomposition processes of forest litter, *Vibrational Spectroscopy*, **19**, 413-417.

Hamby D., (1996), Site remediation techniques supporting environmental restoration activities-a review, *Science of The Total Environment*, **191**, 203-224.

He X., Zhou Y., Wang L., Gu Q., Li F., (2008), Study on influencing factors in removal of volatile organic compounds from red earth by soil vapor extraction, *Journal of Environmental Engineering*, **2**, 238-242.

Hu R., Xiao J., Wang H., Chen G., Chen L., Tian X., (2020), Engineering of phosphate-functionalized biochars with highly developed surface area and porosity for efficient and selective extraction of uranium, *Chemical Engineering Journal*, **379**, http://doi.org/10.1016/j.cej.2019.122388.

Huang M., Zhu Y., Li Z., Huang B., Luo N., Liu C., Zeng G., (2016), Compost as a soil amendment to remediate heavy metal-contaminated agricultural soil: mechanisms, efficacy, problems, and strategies, *Water, Air, and& Soil Pollution*, **227**, 359, http://doi.org/10.1007/s11270-016-3068-8.

Islam M., Jo Y., Park J., (2014), Subcritical water remediation of petroleum and aromatic hydrocarbon-contaminated soil: a semi-pilot scale study, *Water, Air, and Soil Pollution*, **225**, 2037, http://doi.org/10.1007/s11270-014-2037-3.

Jiao W., Han Z., Lyu Z., Ma D., Hu J., Tian Y., (2019), Key issue and expectation of soil electrical resistance heating remediation technology, *Journal of Environmental Engineering*, **13**, 2027-2036.

Leuser R., Velazquez L., Cohen A., Janssen J., (1990), Remediation of PCB soil contamination by on-site incineration, *Journal of Hazardous Materials*, **25**, 375-385.

Li J., Zheng H., Lin X., Zhang X., Wang J., Li T., Zhang Q., (2019), Preparation of three dimensional hydroxyapatite nanoparticles/poly(vinylidene fluoride) blend membranes with excellent dye removal efficiency and investigation of adsorption mechanism, *Chinese Journal of Polymer Science*, **37**, 1234-1247.

Li X., (2018), *Process design and research on operating parameters of thermally enhanced SVE method to repair hydrocarbon contaminated soil*, PhD Thesis, Beijing Institute of Petrochemical Technology.

Li X., Zhu L., Xiao N., Wang Y., (2017), Effect of thermal enhanced SVE on hydrocarbon-contaminated soil remediation, *Industrial Safety and Environmental Protection*, **43**, 101-106.

Ly S., Vong S., Cavailler P., Mumford E., Mey C., Rith S., Buchy P., (2016), Environmental contamination and risk factors for transmission of highly pathogenic avian influenza A (H5N1) to humans, *Cambodia*, *BMC Infectious Diseases*, **16**, 2006-2010.

Ma Y., Zheng X., Feng X., Liu A., Wu Z., (2011), Study on influence factors of soil vapor extraction restoring oil-contaminated soil, *Non-Metallic Mines*, **34**, 53-58.

Mcalexander B., Krembs F., Cardeñosa M., (2015), Treatability testing for weathered hydrocarbons in soils: Bioremediation, soil washing, chemical oxidation, and thermal desorption, *Soil and Sediment Contamination: An International Journal*, **24**, 882-897.

Mora V., Madueño L., Peluffo M., Rosso J., Del Panno M., Morelli I., (2014), Remediation of phenanthrene-contaminated soil by simultaneous persulfate chemical oxidation and biodegradation processes, *Environmental Science and Pollution Research*, **21**, 7548-7556.

Pop D., Micle V., Sur I., (2018), Optimizing the process of depollution through thermal absorption of soils contaminated with crude oil, *Environmental Engineering and Management Journal*, **17**, 2619-2626.

Poppendieck D., Loehr R., Webster M., (1999), Predicting hydrocarbon removal from thermally enhanced soil vapor extraction systems, *Journal of Hazardous Materials*, **69**, 81-93.

Tsitonaki A., Petri B., Crimi M., Mosbaek H., Siegrist R., Bjerg P., (2010), In situ chemical oxidation of contaminated soil and groundwater using persulfate: a review, *Critical Reviews in Environmental Science and Technology*, **40**, 55-91.

Valavanidis A., Vlahogianni T., Dassenakis M., Scoullos M., (2006), Molecular biomarkers of oxidative stress in aquatic organisms in relation to toxic environmental pollutants, *Ecotoxicology and Environmental Safety*, **64**, 178-189.

Volkmar K., Hu Y., Steppuhn H., (1998), Physiological responses of plants to salinity: a review, *Canadian Journal of Plant Science*, **78**, 19-27.

Wang W., Hao Q., Lei W., Xia X., Wang X., (2012), Graphene/sno2/polypyrrole ternary nanocomposites as supercapacitor electrode materials, *Rsc Advances*, **2**, 10268-10274.

Wang Z., (2018), Study on desorption kinetics of different hypercrosslinked resins, *Guangzhou Chemical Industry*, **46**, 63-67.

Yu Y., Liu L., Shao Z., Ju T., Sun B., Benadda B., (2015), A soil-column gas chromatography (SCGC) approach to explore the thermal desorption behavior of hydrocarbons from soils, *Environmental Science and Pollution Research*, **23**, 683-690.

Yu Y., Liu L., Yang C., Kang W., Yan Z., Zhu Y., Wang J., Zhang H., (2019), Removal kinetics of petroleum hydrocarbons from low-permeable soil by sand mixing and thermal enhancement of soil vapor extraction, *Chemosphere*, **236**, 134319, doi: 10.1016/j.chemosphere.2019.07.050.

Yu Y., Shao Z., Liu L., Wen W., Yan Z., (2017), Factors influencing remediation of semi-volatile petroleum hydrocarbon-contaminated soil by thermally enhanced soil vapor extraction, *Journal of Environmental Engineering*, **11**, 2522-2527.

Zhang Z., Liu J., Feng L., Zou W., (2011), A prediction model based on Langmuir theory for equilibrium adsorption amount, *Journal of Northeastern University (Natural Science)*, **5**, 749-751.

Zhu L., Zhang X., Zhu L., Li X., Meng L., (2013), Synthesis and characterization of mesoporous alumina, and adsorption performance for n-butane, *Research on Chemical Intermediates*, **41**, 3637-3648.

Zhao C., Dong Y., Feng Y., Li Y., Dong Y., (2019), Thermal desorption for remediation of contaminated soil: a review, *Chemosphere: Environmental Toxicology and Risk Assessment*, **221**, 841-855.